

**Biaxial nematic phases and V-shaped molecules: A Monte Carlo simulation study**Martin A. Bates<sup>1,\*</sup> and Geoffrey R. Luckhurst<sup>2</sup><sup>1</sup>*Department of Chemistry, University of York, York YO10 5DD, United Kingdom*<sup>2</sup>*School of Chemistry and Southampton Liquid Crystal Institute, University of Southampton, Southampton SO17 1BJ, United Kingdom*

(Received 9 June 2005; published 3 November 2005)

Inspired by recent claims that compounds composed of V-shaped molecules can exhibit the elusive biaxial nematic phase, we have developed a generic simulation model for such systems. This contains the features of the molecule that are essential to its liquid crystal behavior, namely the anisotropies of the two arms and the angle between them. The behavior of the model has been investigated using Monte Carlo simulations for a wide range of these structural parameters. This allows us to establish the relationship between the V-shaped molecule and its ability to form a biaxial nematic phase. Of particular importance are the criteria of geometry and the relative anisotropy necessary for the system to exhibit a Landau point, at which the biaxial nematic is formed directly from the isotropic phase. The simulations have also been used to determine the orientational order parameters for a selection of molecular axes. These are especially important because they reveal the phase symmetry and are connected to the experimental determination of this. The simulation results show that, whereas some positions are extremely sensitive to the phase biaxiality, others are totally blind to this.

DOI: [10.1103/PhysRevE.72.051702](https://doi.org/10.1103/PhysRevE.72.051702)

PACS number(s): 64.70.Md, 61.30.Cz

**I. INTRODUCTION**

In 1970, Freiser showed that deviations from cylindrical symmetry of mesogenic molecules should result in the formation of a biaxial nematic phase, in addition to the conventional uniaxial nematic [1]. The molecular shape considered by Freiser was lath-like, in keeping with the elongated structures of molecules known, at the time, to constitute nematogens. Subsequently, more exotic shapes formed by fusing rods and discs were proposed as likely candidates for the formation of a biaxial nematic [2]. Several studies of the nematic phases formed by such target molecules have reported their biaxiality [3], but it would seem that none of these claims to have found a thermotropic biaxial nematic are correct [4]. Indeed, theory predicts that the biaxial nematic phase can exist only over a very narrow range of molecular biaxialities before it is lost by the sample freezing or by the formation of a smectic phase [5].

An alternative strategy with which to create biaxial molecules is to link two rod-like arms to produce a V-shaped molecule. The nematic phase behavior of such a molecular structure has been investigated with two quite different models using different theoretical approaches: one based on repulsive interactions with a bifurcation analysis [6] and the other using a continuous potential described by a molecular field approximation [4]. Both predict the formation of uniaxial and biaxial nematic phases. In particular, for both theoretical models [4,6], in which the mesogenic arms are equivalent, the Landau point, at which the isotropic phase undergoes a transition directly to the biaxial nematic, is predicted to occur when the link between the arms is at the tetrahedral angle. Such theoretical predictions have been only partly supported by a limited number of computer

simulation studies of bent, hard spherocylinders [7,8]. These simulation models tend to exhibit a uniaxial nematic phase when the angle is large with the density at the *N-I* transition decreasing with the increasing angle. The simulations for bent molecules with shorter arms [7] also reveal the formation of pairs of molecules locked together when the angle between the arms of the V-shaped molecule is smaller than 120°; this is found to preclude the formation of liquid crystal phases directly from the isotropic phase. The formation of such pairs is not accounted for in the theories and these predict a significant variation in the phase behavior from that observed for the hard spherocylinder model. For V-shaped models with long thin arms (where each arm has an aspect ratio of over 5:1 [8]), the biaxial nematic phase is not observed, presumably because of the stability of smectic phases in hard spherocylinder systems which intervene before the minor axis undergoes an orientational transition.

At an experimental level, there has been considerable interest in the liquid crystal phases formed by V-shaped molecules since Niori *et al.* [9] found that they exhibit unusual smectic phases with ferroelectric and antiferroelectric properties. Unfortunately, such materials do not usually exhibit nematic phases and so it was not possible to test the theoretical predictions for the biaxial nematic phase. However, Samulski and his colleagues [10] had been preparing a range of V-shaped molecules to explore the extent to which a molecule might deviate from linearity and still retain its liquid crystallinity. Many of the V-shaped molecules which they prepared do exhibit nematic phases and a more recent example [11] showed an optical texture with two brush patterns. This optical texture has been claimed [12] to indicate a biaxial nematic phase but, as Dingemans and Samulski [10] had noted earlier, results from a range of techniques are needed to demonstrate unambiguously the biaxiality of a nematic phase. Four years later, the evidence for a biaxial nematic was to emerge based on a range of techniques

\*Corresponding author.

including deuterium NMR spectroscopy [13] and x-ray scattering [14]. The V-shaped molecules studied by Samulski and his colleagues are symmetric in that both arms are identical. Lehmann and Levin [15] have also obtained some evidence for the possible biaxiality of the nematic phase formed by a symmetric V-shaped molecule, but with lateral chains on the arms to lower the melting point. In addition, Yelamagad *et al.* [16] have investigated the phase behavior of a V-shaped molecule, but this is nonsymmetric with two very different arms, one of which contains a flexible spacer. Optical measurements also suggest that the nematic phase could be biaxial.

In designing V-shaped molecules that should exhibit the elusive biaxial nematic phase, from the theoretical point of view there are two prime parameters that might be thought to control the phase behavior. One is the angle between the two arms and the other is the relative anisotropy of these arms. When the V-shaped molecule is symmetric, different theories agree that the optimal biaxiality is obtained when the angle adopts the tetrahedral value [4,6]. However, the variation of the phase behavior with the angle when the anisotropies of the two arms are inequivalent has not yet been explored. This could be of special importance because when the mesogenic arms are equivalent, the observation of a biaxial nematic is predicted to require that the angle lies within a very narrow range centered on the tetrahedral value [4] and this would appear to rule out many of the central linking groups for possible real biaxial target molecules [10]. To help understand the structure of a V-shaped molecule and its ability to form a biaxial nematic phase, we have developed a simple model that is clearly related to the structure of real V-shaped molecules. The phase behavior of the model together with certain key properties of the nematic phases have been determined using Monte Carlo simulations. In particular, these properties were determined to explore the optimal measurements which could be made in experiments to determine the symmetry of the nematic phases formed in real mesogens.

The layout of this paper is the following. In Sec. II, the model is described together with the Monte Carlo simulations used to investigate its properties. The results of the simulations are given in Sec. III, where they are compared with theory and the few measurements made on the phases of real V-shaped molecules. Our conclusions are presented in Sec. IV.

## II. THE MODEL AND SIMULATIONS

In order to explore the phase behavior of V-shaped molecules as a function of both the angle and the nonsymmetry in the anisotropies of the arms, we have constructed a simple model based on the Lebwohl-Lasher potential [17]. In their lattice model, designed to investigate the behavior of uniaxial nematic phases, uniaxial molecules on neighboring sites ( $i$  and  $j$ ) of a cubic lattice interact via the purely anisotropic potential

$$U_{ij} = -\epsilon P_2(\cos \beta_{ij}) = -\epsilon P_2(\mathbf{u}_i \cdot \mathbf{u}_j), \quad (1)$$

where  $\epsilon$  is an energy scaling parameter,  $\mathbf{u}_i$  is a unit vector describing the orientation of the uniaxial molecule at site  $i$ ,

$\beta_{ij}$  is the angle between the symmetry axes of the molecules, and  $P_2(x) = \frac{3}{2}x^2 - \frac{1}{2}$  is the second Legendre function. The model exhibits a first order transition between an orientationally ordered and an orientationally disordered state as the temperature is varied; it has thus become a simple prototype model for testing theories of ordering in nematic phases, especially as some of the properties found for real nematogens are well predicted by this simple model [18]. To represent V-shaped molecules, we use a simple extension to the uniaxial model in that each lattice site can host two rather than one mesogenic unit. Each molecule, consisting of two rods of type  $A$  and  $B$  joined at a fixed angle, interacts with the six nearest neighbor molecules on the cubic lattice, as in the Lebwohl-Lasher model. The potential between two identical, neighboring molecules can thus be written as a sum over all distinct pairs of rods

$$U_{ij} = - \sum_{\alpha=A,B} \sum_{\beta=A,B} \epsilon_{\alpha\beta} P_2(\cos \beta_{\alpha\beta}), \quad (2)$$

in which the indices  $\alpha$  and  $\beta$  run over the two rods in molecules  $i$  and  $j$ , respectively. Note that the angle  $\beta_{\alpha\beta}$  is between rod  $\alpha$  in molecule  $i$  and rod  $\beta$  in molecule  $j$ , so that  $\beta_{AB} \neq \beta_{BA}$ . For symmetric molecules, the anisotropy in the interactions for each arm is the same and we have  $\epsilon_{AA} = \epsilon_{AB} = \epsilon_{BB}$ . For nonsymmetric molecules, the anisotropy in the interactions for a pair of rods of type  $A$  is different to that for a pair of type  $B$  (i.e.,  $\epsilon_{AA} \neq \epsilon_{BB}$ ) and, for the mixed interaction, we use a Berthelot-like combining rule  $\epsilon_{AB} = \epsilon_{BA} = \sqrt{(\epsilon_{AA}\epsilon_{BB})}$  [19]. To reduce the number of parameters in the model, it is convenient to introduce a scaling parameter for the energy. To do so, we scale the potential by  $\epsilon_{AA}$  and introduce  $\epsilon^* = \epsilon_{AB}/\epsilon_{AA} = \sqrt{(\epsilon_{BB}/\epsilon_{AA})}$ . The temperature is also scaled in the same way, so that  $T^* = k_B T / \epsilon_{AA}$ . Thus, the two variable parameters in the model are  $\theta$ , the fixed angle between the two arms, and  $\epsilon^*$ , which is related to the ratio of the anisotropies in the interactions of the two arms of the V-shaped molecule. We note that, since the arms are labeled arbitrarily, the labels may be switched, and so we expect a symmetry in the phase diagram between  $\epsilon^*$  and  $1/\epsilon^*$ , with a simple scaling resulting for the transition temperatures. We should point out that, due to the symmetry of the interactions in this lattice based model, that there is an equivalence between the angle  $\theta$  and  $180^\circ - \theta$ , and so we have used the unique range of angles from  $90^\circ$  to  $180^\circ$ . It would, of course, be possible to use an off-lattice model to investigate the effect that the use of nonsymmetric arms in a V-shaped molecule has on the phase diagram. However, the use of a lattice model to do this has a number of advantages. Only a very limited number of simulations can be performed if an off-lattice model is used. For example, so far only two very limited studies have been performed for symmetric V-shaped molecules with fixed aspect ratios used for the arms. To determine the full phase diagram for symmetric molecules, a more in-depth study varying both the aspect ratio of the arms and the angle would need to be performed, a two-variable problem that would require a large computational resource to complete. To investigate the influence of nonsymmetry in the arms, a third variable, related to the difference in the length

of the arms, would need to be included in the model and would massively increase the computational power necessary to investigate fully any changes in phase behavior when the arms are changed. In this respect, the spherocylinder model and other possible off-lattice models are different to the lattice model already described, where the energy scaling parameter of one arm can be eliminated by using it as a scaling variable. For the spherocylinder model, even assuming the same fixed diameter for the two arms, three variables are still required to specify the model completely, namely the angle and the lengths of the two arms; doubling the length of both arms would lead to a different model. However, in the simple lattice model described, only two parameters need to be varied and not three, as necessary for the off-lattice models. Moreover, since lattice models are computationally cheap compared to off-lattice models, the large number of simulations necessary when varying two parameters is not prohibitive and so the problem is tractable. The final reason for using a lattice model is more subtle and is based on the fact that liquid crystal models composed of rotating particles at fixed lattice sites cannot, by their very nature, change in their translational structure. This can be used to our advantage since we may probe regions of a phase diagram where off-lattice systems may form a smectic phase or crystallize, thus blocking the phase of interest. Indeed, this seems to be the case for the long thin symmetric arm cylinder model [8] where the uniaxial nematic phase is observed at higher angles and gradually becomes less stable with respect to the isotropic phase, and so is shifted to high densities, as the angle is decreased. However, the smectic phases start to intervene at densities before the second molecular axis starts to order and so the Landau point and biaxial nematic phase is not observed. Of course, for real systems, it may be that finding the biaxial nematic phase is still a difficult task and that the lattice model results cannot simply be mapped onto the phase diagram of real molecules. However, the simple lattice model is still useful because we can investigate whether it is possible to extend the range of the biaxial nematic phase with respect to the less ordered uniaxial nematic and isotropic phases by varying the nature of the arms of the molecule without having to worry about the more ordered phases hiding the effect we are trying to understand. If the biaxial nematic range is found to be more accessible in certain regions of the phase diagram, then this leads to a more appropriate set of parameters to investigate for real systems or further off-lattice models, rather than aiming for the theoretically predicted V-shaped molecules bent at the tetrahedral angle with symmetric arms.

Simulations were performed for a number of parametrizations of the V-shaped molecule model to map out the phase diagram as a function of both  $\epsilon^*$  and  $\theta$ . In the first series, the phase behavior for symmetric V-shaped molecules (i.e.,  $\epsilon^*=1$ ) was explored as a function of the angle  $\theta$  to make comparisons with previous molecular field predictions for the same model [4]. These simulations were then extended to nonsymmetric V-shaped molecules; thus, the phase diagrams, as functions of the angle  $\theta$ , were constructed for  $\epsilon^*=\sqrt{2}$ ,  $\sqrt{3}$ , 2, and  $\sqrt{5}$ . A second series of simulations were run in which  $\theta$  was fixed and  $\epsilon^*$  was varied. The simulations were initially performed on small systems of  $N=10^3$  lattice

sites to obtain approximate transition temperatures, then appropriate simulations were repeated with a large system of  $N=40^3$  lattice sites to locate the transitions more accurately. These larger systems were also used to evaluate the order parameters necessary for the characterization of the phases as well as for comparison with experiment. Monte Carlo trials were made by selecting a site  $i$  at random and then (i) randomly selecting one of the two rods at this site and randomly changing its orientation, subject to the constraint on the angle  $\theta$  between the two rods or (ii) randomly changing the orientation of both rods at site  $i$ , again subject to the angle constraint on  $\theta$ ; these trials correspond to (i) a random rotation about a random rod axis and (ii) a random rotation about a random axis, respectively. Equilibration runs were typically of 20 000–30 000 cycles (where 1 cycle= $N$  trials) and were followed by a production run of 20 000 cycles, although longer runs were used near transitions where appropriate.

The orientational order of a rigid biaxial molecule in a biaxial phase can be characterized at the second rank level by the Cartesian supermatrix  $\mathbf{S}$  with elements [20,21]

$$S_{ab}^{AB} = \langle (3l_{aA}l_{bB} - \delta_{ab}\delta_{AB})/2 \rangle. \quad (3)$$

Here the subscripts  $a$  and  $b$  denote the molecular axes, the superscripts  $A$  and  $B$  indicate the laboratory axes,  $l_{aA}$  is the direction cosine between the molecular axis  $a$  and the laboratory axis  $A$ ,  $\delta_{ab}$  is a Kronecker delta function, and the angular brackets denote an ensemble average. The properties of this supermatrix are described in more detail in Appendix A. All that we need to note here is that when the principal axes of the molecule and the phase are known, the nonzero elements of  $\mathbf{S}$  are  $S_{aa}^{AA}$  where  $a$  is  $x$ ,  $y$ , or  $z$  and  $A$  is  $X$ ,  $Y$ , or  $Z$ . The symmetry axes for the symmetric V-shaped molecules are known; these are (i) the vector joining the two ends of the molecule, (ii) the axis bisecting the interarm angle, and (iii) the axis orthogonal to the molecular plane. It is also of interest to calculate the ordering matrix for the axes parallel to the arms since, as we shall see, these are of relevance to the experimental determination of the phase symmetry. For the nonsymmetric V-shaped molecules, that is, ones with different anisotropies for the two arms, only the axis orthogonal to the plane formed by the two mesogenic arms is a principal axis. Thus, for these molecules, we only calculate the order parameters of the two arms with respect to the directors appropriate to the phase.

The orientations of the directors, that is, the principal axes of the phase, are not known *a priori* during the Monte Carlo simulation and indeed change from configuration to configuration as they are not constrained in any way. To determine these, we use the procedure described by Vieillard-Baron [22]. In this, a  $Q$  tensor is defined for axes set in the molecule, which is analogous to a diagonal matrix of  $\mathbf{S}$ . Thus, for an axis  $a$ ,

$$Q_{aa}^{AB} = \langle (3l_{aA}l_{aB} - \delta_{AB})/2 \rangle, \quad (4)$$

where now the average is taken over a configuration, and  $A$  and  $B$  denote an arbitrary laboratory frame  $X'$ ,  $Y'$ , and  $Z'$ . The matrix is then diagonalized and the resulting eigenvectors give the orientations of the directors. The eigenvalues,

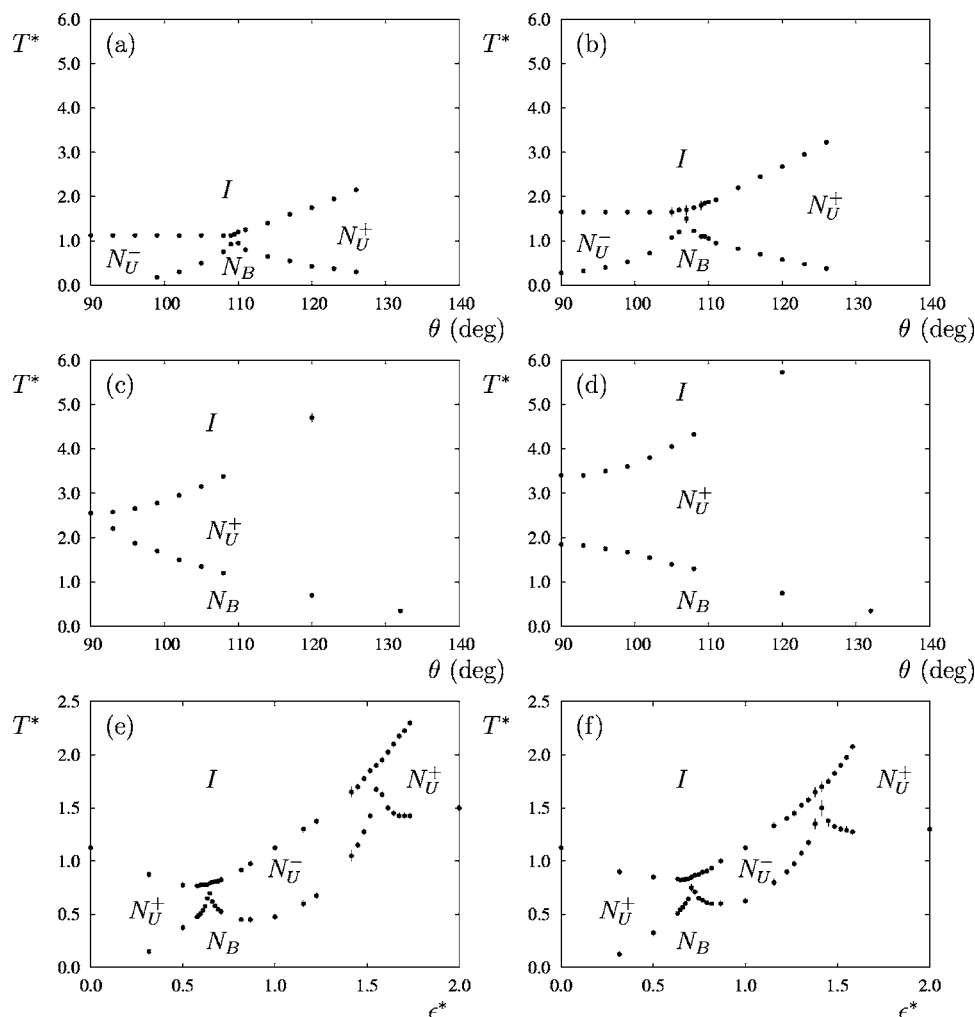


FIG. 1. The phase diagrams for V-shaped molecules as a function of the interarm angle  $\theta$  for a selection of values for the relative anisotropy of the mesogenic groups (a)  $\epsilon^* = 1$ , (b)  $\sqrt{2}$ , (c) 2, and (d)  $\sqrt{5}$  and as a function of the relative anisotropy  $\epsilon^*$  for two values of the interarm angle (e)  $\theta = 105^\circ$  and (f)  $107^\circ$ .

$Q_{aa}^{AA}$  ( $A=X, Y$ , or  $Z$ ), are the order parameters of axis  $a$  with respect to the directors. For a uniaxial phase, the largest order parameter, which is chosen to be denoted  $Q_{aa}^{ZZ}$ , is associated with the unique director along  $Z$  and the other two,  $Q_{aa}^{XX}$  and  $Q_{aa}^{YY}$ , will be equal to  $-\frac{1}{2}Q_{aa}^{ZZ}$  within the simulation error. For a biaxial phase, the three eigenvalues should usually be different; however, for certain molecular axes, they need not be [23]. The order parameters are averaged over many configurations, and in order to maintain a consistent labeling of the principal laboratory axes, we have adopted the procedure proposed by Hashim *et al.* [24]. In this, it is assumed that the orientations of the directors change by only small amounts from one configuration to the next. Consequently, the axes are labeled so that the differences in the orientations of the three principal axes of the phase for a particular configuration with respect to the previous one are minimal.

### III. RESULTS AND DISCUSSION

We begin with the phase behavior of our model nematogen and, in particular, with how the transition temperatures vary with the parameters defining the V-shaped molecule, namely,  $\epsilon^*$  and  $\theta$ . The phases were identified from the orientational order parameters determined for the molecular

symmetry axes and for axes parallel to the arms of the molecule. The transition temperatures were evaluated from the temperature dependence of these. The variation of the transition temperatures with the angle between the mesogenic arms is shown in Figs. 1(a)–1(d) for different values of  $\epsilon^*$ .

The phase diagram for the symmetric V-shaped molecule ( $\epsilon^* = 1$ ) is shown in Fig. 1(a). The smallest interarm angle investigated was  $90^\circ$  and for this fixed angle, the interaction tensor for the molecule is cylindrically symmetric about the axis orthogonal to the arms (see Appendix B) and so may be considered as disk-like. The system forms the isotropic and uniaxial nematic phase. We denote the latter with the conventional  $N_U^-$  notation to indicate the disk-like nature of the molecules. Increasing  $\theta$  does not change the  $N_U^-$ -I transition temperature,  $T_{N_U^-}$ , at least initially. However, a biaxial nematic ( $N_B$ ) as well as the uniaxial nematic is formed when the angle is larger and the  $N_B$ - $N_U^-$  transition temperature does increase quite rapidly with increasing angle. When the V-shaped symmetric molecule is in the tetrahedral geometry ( $\theta = 109.47^\circ$ ,  $\cos^{-1}\theta = -\frac{1}{3}$ ), the isotropic phase is found to undergo a transition directly to the biaxial nematic phase. The appearance of this  $N_B$ -I transition or Landau point at the tetrahedral geometry is in agreement with the prediction of molecular field theory for the symmetric model [4]. As  $\theta$



increases further from  $109.47^\circ$ , the V-shaped molecule becomes more rod-like and again exhibits a uniaxial nematic phase; this is denoted by  $N_U^+$ . Increasing the interarm angle leads to an increase in the  $N_U^+ - I$  transition temperature,  $T_{N_U^+ I}$ . Conversely, as the molecule becomes more uniaxial, so the stability of the biaxial nematic phase is diminished and so  $T_{N_B N_U^+}$  decreases and thus the uniaxial nematic range increases. It is clear from these results that the transition to the biaxial nematic phase for  $\theta = 140^\circ$ , the angle estimated for the symmetric V-shaped molecules studied by Samulski and his colleagues [13], is predicted to occur only after a uniaxial nematic phase with a comparatively long temperature range. In contrast, the real V-shaped molecule appears to undergo a transition to the biaxial nematic phase directly from the isotropic phase or from a uniaxial nematic with a range of just a few degrees. It would seem, therefore, that either this model does not include the anisotropic molecular interactions responsible for the biaxial nematic phase in the real system or that the experimental assignment of the phase is in error.

We now consider how the phase diagram, with its dependence on  $\theta$ , changes with the difference in the anisotropy of the two arms: that is, for an increasingly nonsymmetric V-shaped molecule. The phase diagram shown in Fig. 1(b) is for  $\epsilon^* = \sqrt{2}$ , which would correspond to a factor of 2 in the transition temperatures for the two separate arms (see Appendix B). Perhaps the most obvious change in the phase diagram in comparison with that in Fig. 1(a) is the increase in transition temperatures, although this results simply from an increase in the molecular anisotropy, which in turn results from the fact that  $\epsilon_{AA}$  scales the temperature and  $\epsilon^* = \epsilon_{BB}/\epsilon_{AA}$  is larger than unity. Of course, given the self-duality of the model, a similar phase diagram albeit with different temperature scaling would be obtained if we used a value for  $\epsilon^*$  less than unity (here  $\epsilon^* = 1/\sqrt{2}$ ). There are, however, more subtle and more interesting changes. First, we see that when the arms are orthogonal, a biaxial nematic phase has appeared; this was absent for  $\epsilon^* = 1$ . Second, there is a small shift, of only a few degrees to about  $107^\circ$ , in the interarm angle at which the Landau point occurs. Note that this resulting shift is apparently very small despite the large difference in the nature of the two arms; we recall that, if the mesogens *A* and *B* forming the V-shaped molecules were studied separately, the nematic-isotropic transition temperature for arm *B* would be double that for arm *A*.

The quantitative changes in the phase diagram are found to be even more dramatic for increasing  $\epsilon^*$ . For  $\epsilon^* = \sqrt{3}$ , the Landau point occurs at about  $102^\circ$  and, for the case when the arms are orthogonal, the biaxial nematic range is widened further; thus, the ratio  $T_{N_B N_U^+}/T_{N_U^+ I}$  increases to about 0.44, in comparison to the value 0.17 found for  $\epsilon^* = \sqrt{2}$ . As  $\epsilon^*$  is increased to 2 [see Fig. 1(c)], the Landau point is shifted further across the phase diagram to  $\theta = 90^\circ$ . As the interarm angle is increased from  $90^\circ$ , so the molecular biaxiality is reduced and the biaxial nematic range becomes smaller while the uniaxial nematic range grows as before. Thus, we observe a significant shift in the angle at which the Landau point occurs of almost  $20^\circ$  from the value of  $109.47^\circ$  found

for the symmetric V-shaped molecule by changing the relative nature of the arms. However, we should note that to achieve this shift, the arms in the nonsymmetric molecule must have considerably different anisotropies and that their individual nematic-isotropic transition temperatures would need to differ massively by a factor of 4. Note also that the Landau point is found to be shifted only to lower angles when the relative anisotropy of the arms are changed; thus, using two different arms cannot shift the Landau point to angles larger than the tetrahedral angle.

When the relative anisotropies of the mesogenic arms is increased even further to  $\epsilon^* = \sqrt{5}$ , the variation in the phase behavior again undergoes a dramatic change [see Fig. 1(d)]. Now we see that the system does not exhibit a Landau point, but that the biaxial nematic phase, where it exists, always follows the uniaxial nematic. The  $N_U^+$  phase has the narrowest range when the arms are orthogonal and increases as  $\theta$  increases, which is to be expected as the anisotropy of the V-shaped molecule increases and its biaxiality decreases (see Appendix B).

We have also investigated the phase behavior of the model as a function of the relative anisotropy of the arms for fixed values of the interarm angle. In Fig. 1(e), we show the variation of the phase behavior with  $\epsilon^*$  for a V-shaped molecule with  $\theta = 105^\circ$ . When  $\epsilon^*$  is zero, the molecule is uniaxial and the model mesogen is identical to the Lebwohl-Lasher model [17]. The isotropic phase undergoes a transition to a uniaxial nematic,  $N_U^+$ . As  $\epsilon^*$  increases, that is, the anisotropy of the second arm grows, a biaxial nematic phase appears in the phase diagram, and we observe that  $T_{N_U^+ I}$  falls and  $T_{N_B N_U^+}$  increases. There is a Landau point when  $\epsilon^*$  is approximately 0.64. Note that the Landau point does not occur for the symmetric V-shaped molecule ( $\epsilon^* = 1$ ), because this would require an interarm angle of  $109.47^\circ$ . Thus, it would seem that to compensate for a shift in the interarm angle of less than  $5^\circ$  requires a change in  $\epsilon^*$  from 1 to about 0.64. This difference is consistent with our previous results for  $\epsilon^* = \sqrt{2}$  and  $\sqrt{3}$ . Given the self-dual nature of the model, we expect and observe a second Landau point at  $\epsilon^* = 1.56$ . This value lies between  $\sqrt{2}$  and  $\sqrt{3}$  and, as we have already seen, the Landau points for these two values of  $\epsilon^*$  occur at  $107^\circ$  and  $102^\circ$ , respectively; the consistency with earlier results is clear because  $105^\circ$  is located in this region. The self-dual nature of the model is also apparent from the phase diagram in Fig. 1(e) in that as  $\epsilon^*$  increases from the value at the first Landau point, the relative stability of the biaxial nematic (compared to that of the uniaxial nematic) decreases to a minimum at  $\epsilon^* = 1$  and then increases until at  $\epsilon^*$  of about 1.56 the second Landau point occurs beyond which the  $N_B - N_U^+$  transition temperature again falls. In contrast, over the same  $\epsilon^*$  range, the uniaxial nematic-isotropic transition temperature increases because of the growth in the anisotropy of the second arm of the V-shaped molecule. The appearance of the phase diagram does not change significantly on increasing the interarm angle to  $107^\circ$  as can be seen from the results shown in Fig. 1(f). The most apparent change is in the values at which the Landau points occur. Thus, the relative anisotropy at the first Landau point is about 0.7 and at the second it is its reciprocal, namely 1.4. These values still differ somewhat from the

value of unity found for the symmetric V-shaped molecule with an angle fixed at  $109.47^\circ$ . This significant difference in  $\epsilon^*$  for such a small difference in angle shows just how sensitive the dependence of  $\epsilon^*$  is on  $\theta$  when this is close to the tetrahedral value. In contrast, when  $\theta$  is close to  $90^\circ$ , changes in  $\theta$  have a relatively small effect on the value of  $\epsilon^*$  needed to obtain a Landau point (see also Appendix B, Fig. 6). Indeed, increasing the value of the fixed angle from  $105^\circ$  toward the tetrahedral angle does not change the form of the phase diagram. Initially the two Landau points only approach each other gradually on increasing the angle up to about  $108^\circ$ , then more rapidly after this until they converge at a single point, as we expect, for  $\theta=109.47^\circ$ . For values of the angle above the tetrahedral angle, no Landau point is observed; this is entirely consistent with the results in Figs. 1(a)–1(d) in that no Landau points occur in these phase diagrams above the tetrahedral angle for any values of  $\epsilon^*$ , as noted earlier, and also with the analytic result in Appendix B (see Fig. 6).

The observation that different parametrizations of the model V-shaped molecule exhibit Landau points suggests that the parameters,  $\epsilon^*$  and  $\theta$ , might be mapped onto a single measure of the molecular biaxiality. In addition, it might be expected that the temperature could be scaled with a factor based on both  $\epsilon^*$  and  $\theta$ . These views are supported by the molecular field theory for a nematic formed from flexible molecules where different segments in the molecule interact with the molecular field aligned along the director [25]. It was subsequently shown that the sum of segmental interactions could be written as a single site potential where the interaction tensor depends on the molecular geometry and the strength of the segmental interactions [26]. We expect, therefore, that this will also be the case for the pair potential composed of segmental interactions, and this does indeed prove to be the case, as we shall see. The detailed derivation of the relationship for symmetric and non-symmetric V-shaped molecules is given in Appendix B, where we show that the temperature scaling parameter is given by

$$u_{200} = \frac{3}{32} \epsilon_{AA} \left[ (1 + \epsilon^*) + 3 \left( 1 + \epsilon^{*2} + 4\epsilon^* \left( \cos^2 \theta - \frac{1}{2} \right) \right)^{1/2} \right]^2 \quad (5)$$

and the molecular biaxiality by

$$\lambda = \sqrt{\frac{3}{2}} \left[ \frac{(1 + \epsilon^*) - \left( 1 + \epsilon^{*2} + 4\epsilon^* \left( \cos^2 \theta - \frac{1}{2} \right) \right)^{1/2}}{(1 + \epsilon^*) + 3 \left( 1 + \epsilon^{*2} + 4\epsilon^* \left( \cos^2 \theta - \frac{1}{2} \right) \right)^{1/2}} \right]. \quad (6)$$

The parameters  $u_{200}$  and  $\lambda$  occur in the second rank single site pair potential proposed by Luckhurst *et al.* [27] and used in the first simulation of a biaxial nematic phase [28].

The relationships given in Eqs. (5) and (6) have been applied to all the data for the transition temperatures of the V-shaped molecules presented in Fig. 1. The resulting scaled transition temperatures,  $k_B T / u_{200}$ , are given as a function of

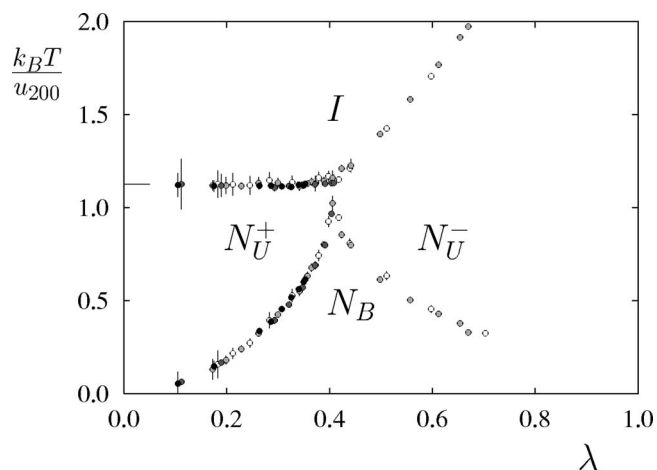


FIG. 2. The phase diagram for all the V-shaped molecules studied as a function of the composite biaxiality parameter  $\lambda$  [see Eqs. (5) and (6)]. Color key: white points,  $\epsilon^* = 1$ ; light grey,  $\epsilon^* = \sqrt{2}$ ; dark grey,  $\epsilon^* = 2$ ; black  $\epsilon^* = \sqrt{5}$ .

the molecular biaxiality  $\lambda$  in Fig. 2. It is immediately apparent that the behavior of all of the V-shaped molecules is contained in a common phase diagram, irrespective of the angle between the arms and their relative anisotropy. The form of the dependence of the phase behavior on  $\lambda$  is consistent with the simulation results of Biscarini *et al.* [29] for the single site potential. At the uniaxial limit,  $\lambda=0$ , the arms of the V-shaped molecule are parallel, and this corresponds to a rod-like molecule. The only ordered phase that this forms is a uniaxial nematic, and this is denoted by the  $N_U^+$  labeling on the phase diagram. The Landau point occurs when  $\lambda = 1/\sqrt{6}$  in keeping with the predictions of the molecular field theory treatment for the single site model [30,31]. For other values of the biaxiality, the uniaxial nematic appears between the isotropic and biaxial nematic phases. The  $T_{N_U^+}$  transition temperature is found to be essentially independent of  $\lambda$ . This is approximately in keeping with molecular field theory, although this predicts a slight increase in  $T_{N_U^+}$  with increasing molecular biaxiality below the Landau point [30,31]. In contrast, the  $N_B$ - $N_U^+$  transition temperature increases rapidly with increasing  $\lambda$  up to the Landau point. The regime where  $\lambda > 1/\sqrt{6}$  corresponds to the angles less than the tetrahedral value for the symmetric V-shaped molecule and so corresponds to a disk-like molecule; we have, therefore, denoted this  $N_U^-$  in Fig. 2. In this regime, the  $N_U^-$ -I transition temperature increases rapidly with  $\lambda$ , while the biaxial nematic decreases in stability. The dependence of  $T_{N_B N_U^-}$  and  $T_{N_U^-}$  on  $\lambda$  is in qualitative agreement with the predictions of the molecular mean field theory [30,31]. We note that even though a common phase diagram exists and all values of  $\epsilon^*$  and  $\theta$  can be mapped on to this, not all values of  $\lambda$  necessarily exist for the two-parameter model in which either  $\epsilon^*$  or  $\theta$  are *a priori* fixed. For example, the phase diagram for  $\epsilon^*=2$  [Fig. 1(c)] maps on to the left hand side of the phase diagram in Fig. 2. A disk-like  $N_U^-$  phase was not observed for this parametrization and, accordingly, none of the points map onto the right hand side of the phase diagram; this, of course, implies that there is no backward mapping for

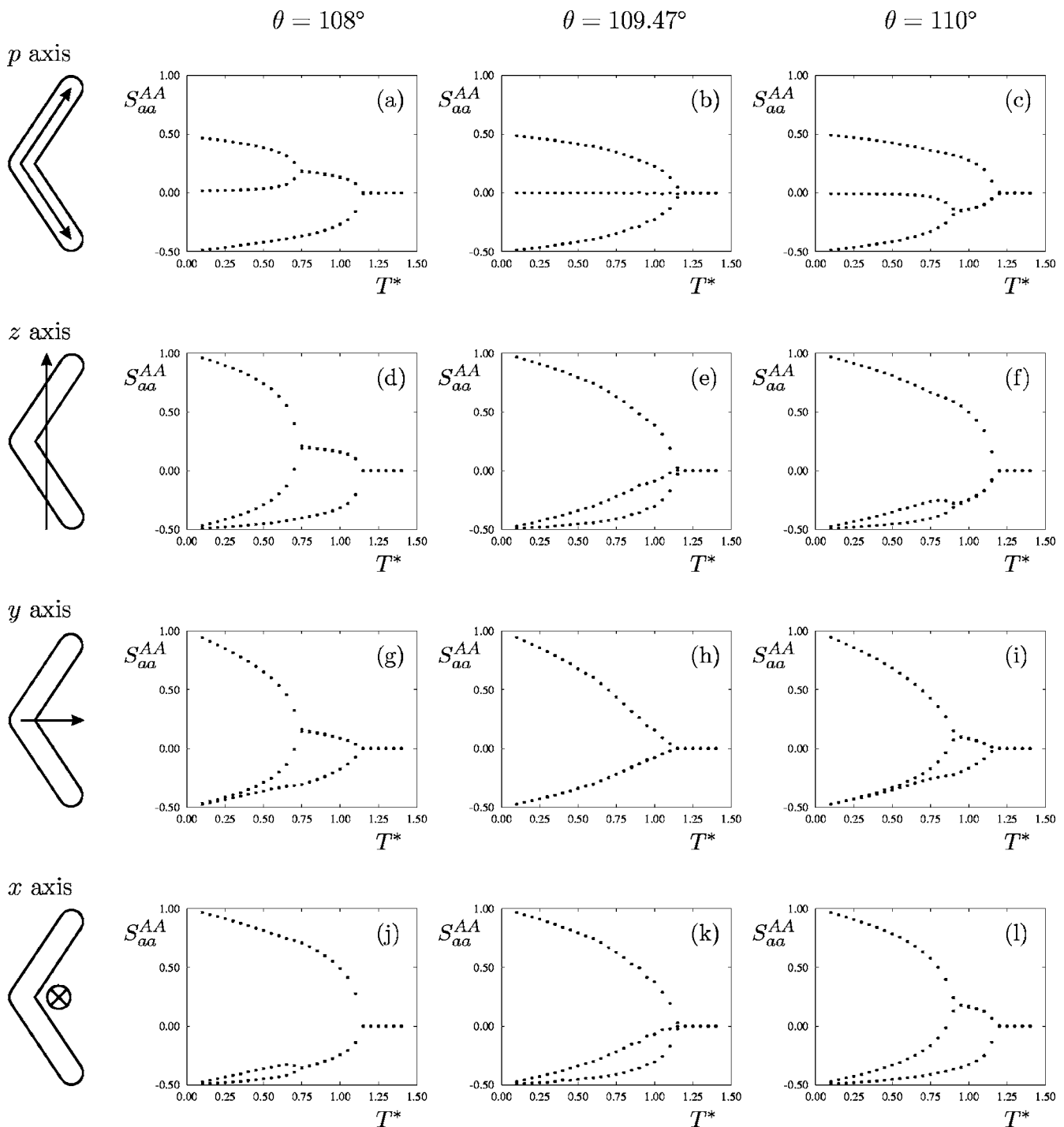


FIG. 3. The temperature dependence of the principal components of the ordering tensor for four axes set in a symmetric V-shaped molecule for three values of the interarm angle  $\theta$ .  $A=X, Y, \text{ or } Z$ ;  $a=p, x, y, \text{ or } z$ .

$\lambda > 1/\sqrt{6}$  onto Fig. 1(c). This, in turn, implies that not all values of  $\lambda$  may be accessible if a particular central linking group for the molecule (i.e.,  $\theta$ ) or similarly a particular pair of arms (i.e.,  $\epsilon^*$ ) is chosen for the target molecule. To aim for a molecule with a particular value of  $\lambda$ , there should be some flexibility in both the choice of  $\theta$  and  $\epsilon^*$ .

We now turn to the second rank orientational order parameters for both the uniaxial and biaxial nematic phases. We start by illustrating our results for three symmetric

V-shaped molecules, having the following interarm angles:  $109.47^\circ$ , for which a Landau point is observed, and  $108^\circ$  and  $110^\circ$ , which are located either side of the Landau point in Fig. 1(a). The phase orientational order parameters have been determined for four different axes set in the molecule. One axis ( $p$ ) is parallel to the mesogenic arm and the other three ( $x, y, \text{ and } z$ ) are parallel to the principal axes of the molecule. Note that, for the axis parallel to the arm, both arms are used to determine the order parameters, since these are equivalent

for the symmetric molecule. For the principal axes, these are determined by the symmetry of the V-shaped molecule and are indicated as  $x$ ,  $y$ , and  $z$  in Fig. 3: axis  $x$  is orthogonal to the plane containing both arms, axis  $y$  bisects the angle in the plane containing the arms, and axis  $z$  is orthogonal to the other two, that is, along the long axis of the molecule, defined by joining the two ends. We have chosen to show the ordering matrices for the individual axes rather than the principal second rank order parameters (see Appendix A) because this permits direct contact with the deuterium NMR experiments usually taken as the most definitive measure of phase biaxiality [4]. In these experiments, the quadrupolar splitting for a deuteron is measured along the three orthogonal directors and these splittings lead to the order parameters  $S_{CD}^{XX}$ ,  $S_{CD}^{YY}$ , and  $S_{CD}^{ZZ}$  for the carbon deuterium (CD) bond with respect to the directors. The experiments, therefore, provide the major order parameter,  $S_{CD}^{ZZ}$ , and the phase biaxiality  $S_{CD}^{XX} - S_{CD}^{YY}$  for different axes in the molecule. Depending on the location of the CD bond, these two order parameters are related to the four principal order parameters, but we shall not be concerned with this specific dependence here (but see Appendix A).

We shall start our discussion with the results for the symmetric V-shaped molecule having an interarm angle of  $110^\circ$  [see Figs. 3(c), 3(f), 3(i), and 3(l)]. As we have seen [see Fig. 1(a)], this forms both uniaxial and biaxial nematic phases. In the uniaxial nematic phase, for each axis there is a unique order parameter,  $S_{CD}^{ZZ}$ , associated with its ordering with respect to the director. The other two order parameters,  $S_{CD}^{XX}$  and  $S_{CD}^{YY}$ , are necessarily the same and equal to  $-\frac{1}{2}S_{CD}^{ZZ}$ . This is seen to be the case for all the molecular axes studied within the uniaxial nematic phase. Thus for  $S_{zz}^{ZZ}$  [see Fig. 3(f)], there is a small jump in its value at the uniaxial nematic-isotropic transition at  $T^* = 1.15$  and the order parameter then grows with decreasing temperature. Its positive value shows that the molecular  $z$  axis tends to align parallel to the director. The other two order parameters associated with alignment perpendicular to the director are, naturally, negative and equal. Consequently, for this value of  $\theta$ , it is reasonable to assume that the molecule is behaving as a rod-like object. The unique order parameters for the  $x$  and  $y$  axes [see Figs. 3(l) and 3(i), respectively] are, in contrast, negative showing that these axes tend to be ordered orthogonal to the director, as expected. The two associated order parameters for the  $x$  and  $y$  axes are necessarily positive and equal within the uniaxial nematic region. Finally, the unique order parameter for the arm axis, which is not a molecular symmetry axis, is positive but relatively small in comparison to that for the  $z$  axis. This is in keeping with the fact that the order parameter for the arm is a linear combination of the principal order parameters

$$S_{pp}^{ZZ} = S_{zz}^{ZZ} \sin^2(\theta/2) + S_{yy}^{ZZ} \cos^2(\theta/2). \quad (7)$$

At the transition from the uniaxial to the biaxial nematic, the unique order parameters continue to change continuously with decreasing temperature. This is in keeping with the second order character of this transition predicted by molecular field theory [30]. The order parameters that are degenerate in the uniaxial nematic phase split apart in the biaxial nematic

phase and so there are three different values of the phase order parameters for each axis. The magnitude of the differences for these order parameters varies significantly according to the molecular axis chosen to define them. The largest biaxiality in the order parameters is exhibited by the arm axis. In fact, just below the  $N_B - N_U^+$  transition, one order parameter  $S_{pp}^{XX}$  is essentially 0 so that the other two order parameters are equal in magnitude, but opposite in sign. In this case, the relative biaxiality determined by the NMR experiments, namely  $(S_{pp}^{XX} - S_{pp}^{YY})/S_{pp}^{ZZ}$ , is close to its maximum possible value of unity. This result is in marked contrast to that found by Madsen *et al.* [13], where the phase biaxiality of the arms of the V-shaped molecule, thought to form a biaxial nematic phase, appears to be very close to 0; however, the interarm angle of  $140^\circ$  is significantly larger than the values that we find necessary to yield a biaxial nematic phase. The  $x$  axis provides the next largest measure of the phase biaxiality, especially in the vicinity of the  $N_B - N_U^+$  transition, where the difference  $(S_{xx}^{XX} - S_{xx}^{YY})$  is large. However, as the temperature is lowered, the phase biaxiality starts to decrease and is observed to tend to 0 as the temperature tends to 0. This occurs as at low temperature,  $S_{xx}^{ZZ}$  tends to unity because the trace of the tensor vanishes and the most negative order parameter is  $-1/2$ . In other words, both  $S_{xx}^{XX}$  and  $S_{xx}^{YY}$  must approach the limit of  $-1/2$ , at which point their difference disappears. Of course, it does not follow that the phase is no longer biaxial in this limit, but simply that the axis used to explore the phase symmetry is inappropriate in this highly ordered limit. The biaxial ordering of the  $y$  axis  $(S_{yy}^{XX} - S_{yy}^{YY})$  is relatively large in the vicinity of the  $N_B - N_U^+$  transition. However, as the temperature is reduced, this difference tends rapidly to 0 even before the major order parameter  $S_{yy}^{ZZ}$  has reached its limiting value of unity. The final molecular symmetry axis is  $z$  and for this we again see a relatively small phase biaxiality  $(S_{zz}^{XX} - S_{zz}^{YY})$  appear at the transition to the biaxial nematic. This biaxiality in the order parameters grows and then decreases tending to the limiting value of 0 as the temperature is reduced.

Similar behavior for the order parameters is observed for the V-shaped molecule with the slightly smaller interarm angle of  $108^\circ$ , which occurs on the other side of the Landau point. We note that since the angle  $108^\circ$  deviates more than  $110^\circ$  from the tetrahedral angle of  $109.46^\circ$ , the uniaxial nematic has a slightly wider range for the smaller angle than for the larger one, and so the exact temperature dependence of the order parameters will differ for the two models; however, the behavior of the order parameters is very similar and may still be compared. The essential difference in the behavior of the order parameters proves to be in the labeling of the molecular axes. Thus, the temperature dependence of the order parameters for axis  $x$  when  $\theta = 108^\circ$  matches that for the  $z$  axis when  $\theta = 110^\circ$ . This exchange of behavior for the different axes suggests that the  $x$  axis is the major molecular axis and, because this is orthogonal to the plane containing the two mesogenic arms, that the molecule is disk-like; this is entirely in keeping with earlier remarks about changing from rod-like behavior on one side of the Landau point to disk-like on the other. The results also show that the ordering of the  $y$  axis is the same for both angles on either side of the



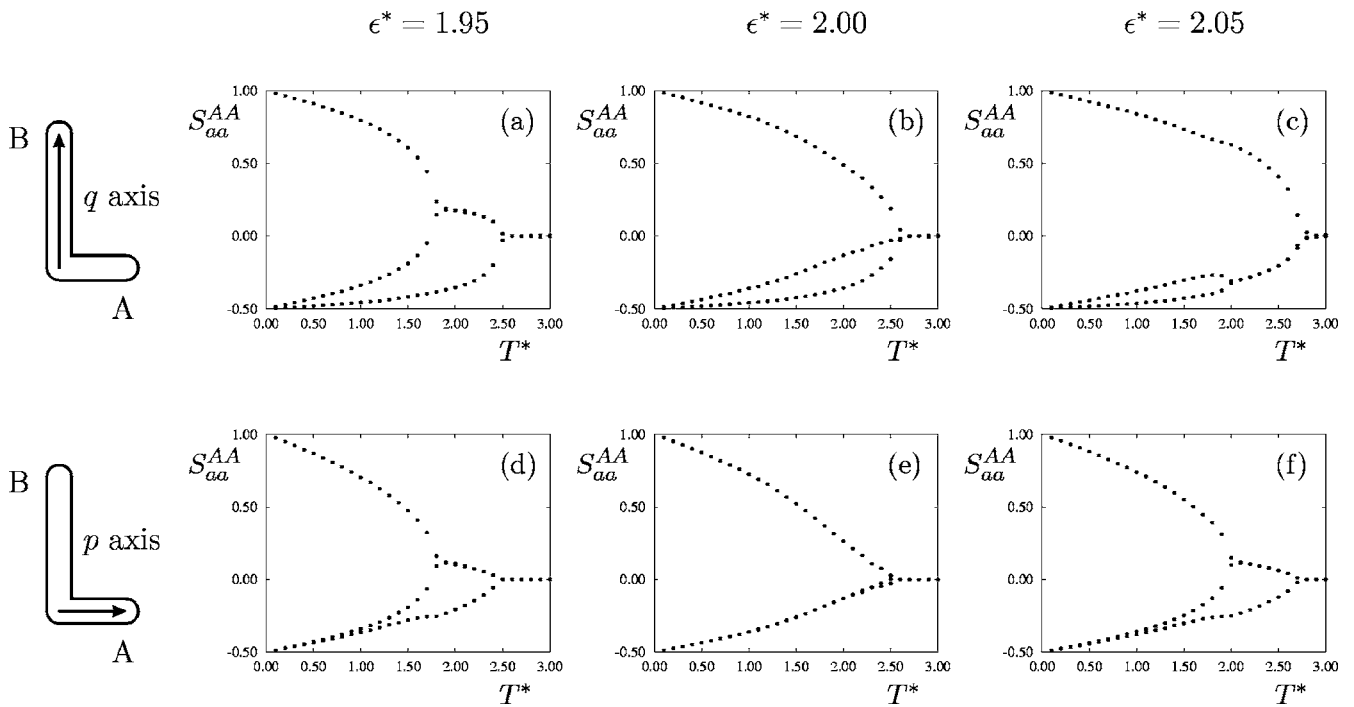


FIG. 4. The temperature dependence of the principal components of the ordering tensor for the two mesogenic arms of an orthogonal, nonsymmetric V-shaped molecule for three values of the relative mesogenic anisotropy  $\epsilon^*$ .  $A=X, Y$ , or  $Z$ ;  $a=p$  or  $q$ .

Landau point. We observe that the order parameters for the arm axis, again, exhibit the maximal biaxiality of about unity, as we found for the larger interarm angle. There is, however, a significant difference in that the single order parameter in the uniaxial nematic phase is negative, thus, revealing the tendency for the molecules to align orthogonal to the director, in keeping with their disk-like character. On entering the biaxial nematic phase, the two small order parameters, which were equivalent in the uniaxial nematic, now become dissimilar with one increasing and the other tending to zero. Thus, the order parameters for the arms of the two V-shaped molecules differ, to a first approximation, simply by a change of sign.

We now come to the special case when the angle between the arms adopts the tetrahedral value, for then the system undergoes a transition directly from the isotropic to the biaxial nematic phase: that is, the system is at the Landau point in the phase diagram. As with the other two geometries, the biaxiality in the order parameters is largest for the arm axis. At the transition to the biaxial nematic phase, one order parameter remains 0, while the other two grow, essentially continuously from the transition, in keeping with the second order character of the  $N_B$ -I transition [30]. Since the two nonzero order parameters are equal and opposite in sign, the relative phase biaxiality determined from the order parameters adopts its maximum value of unity for all temperatures. The  $x$  and  $z$  molecular axes are ordered to equivalent extents, in keeping with the fact that the molecule can no longer be described as either a rod or a disk. At the transition, the biaxiality in these order parameters grows, passes through a maximum, and then decreases with decreasing temperature until it reaches 0 as the major order parameter tends to its limiting value of unity. The order parameters for the molecu-

lar  $y$  axis, which bisects the angle between the two arms, exhibit an especially interesting behavior. First, unlike the order parameters for the other molecular axes, all three order parameters  $S_{yy}^{XX}$ ,  $S_{yy}^{YY}$ , and  $S_{yy}^{ZZ}$  tend to 0 on increasing the temperature with a concave rather than convex curvature. Second, since two of the order parameters are equal, the biaxial order parameter is found to be 0 over the entire temperature range of the biaxial nematic phase. Hints of such behavior are apparent from the results for the same axis in the two V-shaped molecules in which the angle  $\theta$  deviates slightly from the tetrahedral value. For these, the phase biaxial order parameter is seen to vanish over a significant part of the biaxial nematic range. This extreme and intriguing behavior found for the  $y$  axis emphasizes the considerable care that needs to be taken when placing deuterons in a molecule in order to determine the symmetry of a possibly biaxial nematic phase.

We have also investigated the behavior of the order parameters for the case where the V-shaped molecule is nonsymmetric. To study the behavior around the Landau point in this situation, we use three different parametrizations as before, this time fixing the angle  $\theta$  to be  $90^\circ$  and varying the relative anisotropies about the Landau point. For molecules in which the arms are orthogonal, the Landau point occurs for  $\epsilon^*=2$  [see Fig. 1(c) and Appendix B]. We have, therefore, studied this value and also two values on either side of the Landau point: namely,  $\epsilon^*=1.95$  (disk-like) and  $\epsilon^*=2.05$  (rod-like). As these molecules are nonsymmetric, we only calculate the order parameters for the two arms, but this time do not average them as for the symmetric case; instead, we define vectors  $p$  along arm  $A$  and  $q$  along arm  $B$ . These are shown for the three models as a function of temperature in Fig. 4. As we shall see, the behavior observed is analogous to

that for the V-shaped molecule with tetrahedral and near tetrahedral geometry. This is perhaps to be expected given the equivalence of the pair potentials for particular geometries and anisotropies of the V-shaped molecule demonstrated in Appendix B. In consequence, the comments on the results for the systems with orthogonal mesogenic arms will be kept relatively brief.

We shall start with the V-shaped molecule having the largest relative anisotropy,  $\epsilon^* = 2.05$  [see Figs. 4(c) and 4(f)]. This exhibits both uniaxial and biaxial nematic phases. In the uniaxial phase, the unique order parameter for arm *B* is positive, indicating its tendency to align parallel to the director. Accordingly, arm *A* tends to be aligned orthogonal to the director and so its unique order parameter is negative. At the transition to the biaxial nematic phase, the equivalence of the remaining pairs of order parameters is removed. For axis *B*, the resulting biaxiality in the order parameters ( $S_{qq}^{xx} - S_{qq}^{yy}$ ) is small, grows slightly, and then decreases to the limiting value of zero; this is similar to the behavior observed for the *z* axis for the symmetric V-shaped molecule with  $\theta = 110^\circ$ . In contrast, the separation of the order parameters for the *A* axis is considerable with one order parameter positive and increasing to unity while the other decreases, becoming negative and reaches the limiting value of  $-1/2$  at low temperatures. The phase biaxiality, therefore, starts at zero at the transition, goes through a relatively large maximum compared to that for arm *B*, but then decreases to zero; this is similar to the *y* axis for the  $110^\circ$  symmetric molecule.

For the molecule with the slightly smaller anisotropy,  $\epsilon^* = 1.95$ , just less than that needed for the optimum molecular biaxiality, the results for the order parameters for the two arms are shown in Figs. 4(a) and 4(d). The results for the ordering of the arm *A* is essentially the same for both anisotropies: in keeping with the similar behavior for the *y* axis of both the  $108^\circ$  and  $110^\circ$  symmetric molecules. However, the order parameters for arm *B* are quite different in both the uniaxial and biaxial nematic phases. In the uniaxial nematic, this arm tends to be aligned orthogonal to the director because of the change in the total interaction tensor when  $\epsilon^*$  changes from 2.05 to 1.95 (see Appendix B); thus, the molecule is behaving more like a disk than a rod. Within the biaxial nematic phase, the biaxial ordering of arm *B* increases rapidly at the transition, but then decreases to 0 at low temperatures. This again contrasts with the ordering of the equivalent arm when the relative anisotropy for the arms of the V-shaped molecule increases just slightly to  $\epsilon^* = 2.05$ . The order parameters for the optimal molecular biaxiality are shown in Figs. 4(b) and 4(e). The ordering of arm *A* for this system is identical to that of axis *y* for the symmetric V-shaped molecule with the tetrahedral geometry [see Fig. 3(h)]. In other words, there is no biaxiality in the ordering for this arm over the entire range of the biaxial nematic. The ordering of arm *B* does exhibit a small phase biaxiality which is comparable to that of axis *z* in the symmetric tetrahedral V-shaped molecule. This again indicates the care that needs to be taken over where deuterons are placed in the molecule when using NMR to investigate the symmetry of the phase. For the symmetric tetrahedral V-shaped molecule, the best

place to place a CD bond is along the arm axis. In contrast, if a CD bond is placed along the *A* arm for the optimal biaxial orthogonal molecule, no biaxiality in the ordering is observed.

#### IV. CONCLUSIONS

Based on the Lebwohl-Lasher model for uniaxial nematics, we have developed a generic model for the anisotropic interactions between V-shaped molecules, which is directly related to their structure. The defining characteristics are the anisotropies of the two arms and the angle between them. For the symmetric V-shaped molecule, the phase behavior is determined solely by the interarm angle. When this is  $109.47^\circ$ , the tetrahedral angle, the isotropic phase undergoes a transition directly to the biaxial nematic in agreement with the prediction of molecular field theory. In addition, the predicted strong dependence of the stability of the biaxial nematic phase on the angle when it is close to the tetrahedral value has been confirmed. The V-shaped molecule can also be nonsymmetric, which introduces a new element into the design of compounds capable of forming a biaxial nematic. The effect of the difference in the anisotropies of the two groups on the phase behavior is to shift the angle at which the Landau point occurs to lower values. However, if the relative anisotropy for the arms is greater than 2, then there is no angle which gives a Landau point and the biaxial nematic phase necessarily follows a uniaxial phase.

The model clearly contains three parameters: the anisotropies of the two arms and the angle between them. However, one of the anisotropies can be used to scale the temperature, which leaves the relative anisotropy and the interarm angle to control the phase behavior of the model. It proves to be possible to combine these two parameters into a single measure of the biaxiality in the molecular interactions. In addition, the temperature scaling can also be replaced by a function of both the interarm angle and their relative anisotropy. Use of these two parameters allows all of our results to be presented in a single phase diagram, identical to that for a single site biaxial potential. The excellent agreement for all of the V-shaped molecules studied provides a uniquely accurate version of this phase diagram. In addition, this can now be used to determine the phase behavior for any analogous model nematogen composed of interacting segments. This route is especially useful for comparing real molecules to the single phase diagram. While it is relatively easy to estimate the values of  $\epsilon^*$  and  $\theta$  for a particular molecule and use the mapping detailed here to transfer them to the single phase diagram, it is not so straightforward to consider designing a molecule with a particular  $\lambda$  value without using such a mapping.

The simulations were also used to explore the orientational order of the uniaxial and biaxial nematic phases formed by the V-shaped molecules. The order parameters needed to do this were defined in terms of various axes set in the molecule and the directors characterizing the phase. Such quantities are of special importance in helping to determine

the symmetry of the phase and so identifying it, either as a uniaxial or biaxial nematic. For symmetric V-shaped molecules, the order parameters for the molecular symmetry axes and the arms were determined. By far the best indicator of the phase symmetry was found to be the arm axis and for this, the relative biaxiality in its order parameters was close to the maximal value of unity. In contrast, the relative biaxiality was found to be zero over much of the biaxial nematic range when the order parameters for the axis bisecting the arms was used. Indeed, for the tetrahedral geometry, the biaxiality is zero over the entire biaxial nematic range. For the case of an orthogonal V-shaped molecule with optimal biaxiality ( $\theta=90^\circ$ ,  $\epsilon^*=2$ ), placing the CD bond along the axis of the arm with higher anisotropy is a reasonable indicator of phase biaxiality; however, placing the CD bond along the other arm axis leads to zero biaxiality in the order parameters. These results are of special importance for those experimentalists using deuterium NMR spectroscopy to determine the phase symmetry, for it shows that extreme care must be taken in locating the deuterons if this method is to be used successfully. Finally, we note that the order parameters seem to change continuously at the biaxial nematic–uniaxial nematic transition and at the Landau point, in keeping with the predicted second order character of these transitions.

#### ACKNOWLEDGMENT

M.A.B. is grateful to the Royal Society for both financial support and for funding the computer cluster to simulate these systems.

#### APPENDIX A

The second rank Cartesian supermatrix  $\mathbf{S}$  used to characterize the orientational order of a biaxial molecule in a biaxial phase is defined in Eq. (3). Here we describe some of the properties of  $\mathbf{S}$  and propose a particular notation for it. In general, the supermatrix contains 81 nonzero elements, but the number of independent elements is just 25. This follows because the exchange of the direction cosines,  $l_{aA}$  and  $l_{bB}$ , leaves the supermatrix elements unchanged and the properties of the direction cosines requires that the trace of each submatrix vanishes. The number of independent components is clearly significant, but can be reduced if the principal axes for both the phase and the molecular matrices are known. This leaves the nine diagonal elements,  $S_{aa}^{AA}$ , as nonzero and, because  $\sum_a S_{aa}^{AA}$  and  $\sum_A S_{aa}^{AA}$  both vanish, we are left with just four independent elements of the ordering supermatrix. In a simulation, the orientations of the principal axes of the biaxial phase can be determined and the molecular principal axes are usually available from the model potential. In contrast, the location of both sets of axes for real mesogens presents experimentalists with a considerable challenge. This is especially true for the principal axes of the molecule because of the flexibility of mesogenic molecules and the absence of symmetry for the conformational states. The use of probe molecules to explore the phase symmetry presents fewer problems because rigid probes of high symmetry can be used.

The combination of the four independent principal components of  $\mathbf{S}$  to represent the orientational order of a biaxial molecule in a biaxial phase is given by Dunmur and Toriyama [21]. They use the following notation:

$$S = S_{zz}^{ZZ}, \quad D = S_{xx}^{ZZ} - S_{yy}^{ZZ}, \quad P = S_{zz}^{XX} - S_{zz}^{YY},$$

$$C = (S_{xx}^{XX} - S_{xx}^{YY}) - (S_{yy}^{XX} - S_{yy}^{YY}). \quad (\text{A1})$$

The first two order parameters,  $S$  and  $D$ , are nonzero in both uniaxial and biaxial phases. They reflect the orientational order of the molecular axes with respect to the director  $\hat{\mathbf{n}}$ , which is parallel to  $Z$ . The other two,  $P$  and  $C$ , vanish in the uniaxial phase and are nonzero in the biaxial phase. Of these,  $P$  is a direct measure of the biaxial ordering of the  $z$  molecular axis with respect to the laboratory axes,  $X$  and  $Y$ , along which the  $\hat{\mathbf{l}}$  and  $\hat{\mathbf{m}}$  directors are parallel. The other biaxial order parameter  $C$  is the difference in the phase biaxiality observed for the  $x$  and  $y$  molecular axes. In the limit of high orientational order,  $S$  tends to 1, while  $C$  tends to 3, in contrast, both  $D$  and  $P$  tend to zero.

Other letters have been used to denote the four independent order parameters constructed as linear combinations of the principal components of  $\mathbf{S}$ . This is undesirable as is the fact that the letters are not related in any transparent manner to the particular linear combination of  $S_{aa}^{AA}$  that they denote. We suggest a solution to this based on the use of Wigner rotation matrices,  $D_{MN}^L(\Omega)$ , to describe the orientational order of a biaxial molecule in a biaxial phase. This solution is based on work by Straley [31], who averaged functions of the Euler angles,  $\Omega(\equiv\alpha\beta\gamma)$ , to define the four independent order parameters; these are

$$S = \langle (3 \cos^2 \beta - 1)/2 \rangle,$$

$$U = \langle (\sin^2 \beta \cos 2\gamma) \rangle,$$

$$T = \langle (\sin^2 \beta \cos 2\alpha) \rangle,$$

$$V = \langle \frac{1}{2}(1 + \cos^2 \beta) \cos 2\alpha \cos 2\gamma - \cos \beta \sin 2\alpha \sin 2\gamma \rangle. \quad (\text{A2})$$

Another variation of these order parameters has recently been proposed by Sonnet *et al.* [32]. Their order parameters are defined by

$$S = \langle (3 \cos^2 \beta - 1)/2 \rangle,$$

$$S' = \frac{3}{2} \langle (\sin^2 \beta \cos 2\gamma) \rangle,$$

$$T = \frac{1}{2} \langle (\sin^2 \beta \cos 2\alpha) \rangle,$$

$$T' = \langle \frac{1}{2}(1 + \cos^2 \beta) \cos 2\alpha \cos 2\gamma - \cos \beta \sin 2\alpha \sin 2\gamma \rangle. \quad (\text{A3})$$

Both sets of functions are proportional to linear combinations of the second rank Wigner rotation matrices,  $D_{mn}^2(\Omega)$ , defined by

$$R_{mn}^2(\Omega) = \frac{1}{4} \delta_{m,\text{even}} \delta_{n,\text{even}} \{D_{mn}^{2*}(\Omega) + D_{-mn}^{2*}(\Omega) + D_{m-n}^{2*}(\Omega) + D_{-m-n}^{2*}(\Omega)\}, \quad (\text{A4})$$

chosen because of the effective  $D_{2h}$  symmetry of the phase and of the molecules [33]. They are analogous to those defined by Mulder [34] when considering the interaction between a pair of molecules with  $D_{2h}$  symmetry. Here  $m$  and  $n$  are defined to be positive and the four order parameters are given by

$$\begin{aligned} \langle R_{00}^2 \rangle &= S, & \langle R_{20}^2 \rangle &= \sqrt{\frac{3}{8}} T, \\ \langle R_{02}^2 \rangle &= \sqrt{\frac{3}{8}} U, & \langle R_{22}^2 \rangle &= V/2, \end{aligned} \quad (\text{A5})$$

and evaluation of the direction cosines in terms of the Euler angles shows that [21]

$$\begin{aligned} S &= \langle R_{00}^2 \rangle, & D &= \sqrt{6} \langle R_{02}^2 \rangle, \\ P &= \sqrt{6} \langle R_{20}^2 \rangle, & C &= 6 \langle R_{22}^2 \rangle. \end{aligned} \quad (\text{A6})$$

In view of this direct proportionality between the Cartesian representation of the orientational order parameters and the averages of the  $R_{mn}^2(\Omega)$  functions, we suggest that the combinations of the principal components of the Cartesian supermatrix are denoted as follows:

$$\begin{aligned} S_{00}^2 &= S_{zz}^{ZZ}, & S_{02}^2 &= S_{xx}^{ZZ} - S_{yy}^{ZZ}, \\ S_{20}^2 &= S_{zz}^{XX} - S_{zz}^{YY}, \\ S_{22}^2 &= (S_{xx}^{XX} - S_{xx}^{YY}) - (S_{yy}^{XX} - S_{yy}^{YY}). \end{aligned} \quad (\text{A7})$$

These definitions use the letter  $S$  to represent the orientational order parameters as this is already widely adopted in the field. The superscript 2 denotes the fact that these are second rank orientational order parameters. The subscripts have the following meanings: 00 denotes the ordering of the molecular  $z$  axis with respect to  $Z$ ; 02 indicates the difference in the ordering of the laboratory  $Z$  axis with respect to the molecular  $x$  and  $y$  axes; conversely, its laboratory counterpart, 20 denotes the difference in the ordering for the molecular  $z$  axis with respect to the laboratory  $X$  and  $Y$  axes; and finally, 22 indicates the differences in the ordering of the molecular  $x$  and  $y$  axes with respect to the laboratory  $X$  and  $Y$  axes.

## APPENDIX B

The segmental model that we have developed for the anisotropic potential between two symmetric V-shaped molecules based on second rank interactions proves to be equivalent to a single site potential, also of second rank [35]. The demonstration of this is based on a formal, geometric relationship between the direction cosines occurring in the segmental pair potential [see Eq. (2)] and those describ-

ing the orientations of the molecular symmetry axes. Here, we give an alternative, more physical, derivation which is readily applicable not only to symmetric V-shaped molecules, but also to their nonsymmetric analogues that we have investigated. In the single site model, the anisotropic pair potential can be written as

$$U_{ij} = \sum_{m,n} u_{2mn}^{ij} D_{mn}^2(\Omega_{ij}), \quad (\text{B1})$$

where  $\Omega_{ij}$  denotes the Euler angles relating axis systems set in molecules  $i$  and  $j$  [27]. The dependence on the molecular orientation with respect to the intermolecular vector has been projected out from the total potential [27]. The strength of the anisotropic potential is contained in the expansion coefficients,  $u_{2mn}^{ij}$ , which constitute a supertensor. In the principal axis systems of the two molecules, there are just three nonzero coefficients,  $u_{200}^{ij}$ ,  $u_{220}^{ij} (\equiv u_{202}^{ij})$ , and  $u_{222}^{ij}$ , but these can be related by invoking a Berthelot-like combining rule [27]

$$u_{220}^{ij} = (u_{200}^{ij} u_{222}^{ij})^{1/2}. \quad (\text{B2})$$

The ratio,  $u_{220}^{ij}/u_{200}^{ij}$ , reflects the relative biaxiality  $\lambda$  of the anisotropic interactions. This combining rule is consistent with writing the intermolecular supertensor in terms of molecular tensors for the individual molecules [27], that is

$$u_{2mn}^{ij} = u_{2m}^i u_{2n}^j. \quad (\text{B3})$$

This result certainly holds for anisotropic dispersion forces, but is more general than this. The biaxiality parameter  $\lambda$  may now be written in terms of molecular quantities as

$$\lambda = u_{22}^i / u_{20}^i. \quad (\text{B4})$$

As we are considering only single component systems, this ratio is the same for all molecules, and so the label  $i$  will be removed for the remainder of this appendix. The two components of the irreducible spherical tensor are related to those of the Cartesian tensor by

$$u_{20} = \sqrt{\frac{3}{2}} u_{zz} \quad (\text{B5})$$

and

$$u_{22} = \frac{1}{2} (u_{xx} - u_{yy}), \quad (\text{B6})$$

where  $x$ ,  $y$ , and  $z$  denote the principal axis system for  $\mathbf{u}$ , which is traceless.

The interaction tensor,  $u_{2m}$ , is the tensorial sum of the segmental tensors  $\mathbf{u}_A$  and  $\mathbf{u}_B$ , where  $A$  and  $B$  are the two arms. We start by evaluating this sum for a nonsymmetric V-shaped molecule in the arbitrary coordinate system shown in Fig. 5. Here  $z$  is parallel to the arm  $A$ ,  $x$  is orthogonal to  $z$  and in the plane formed by the two arms, and  $y$  is orthogonal to this plane. In this coordinate system, the Cartesian components of the total tensor are



$$\begin{pmatrix} \frac{1}{2}[-u_A + u_B(3 \sin^2 \theta - 1)] & 0 & \frac{3}{2}u_B \cos \theta \sin \theta \\ 0 & -\frac{1}{2}(u_A + u_B) & 0 \\ \frac{3}{2}u_B \cos \theta \sin \theta & 0 & \frac{1}{2}[u_A + u_B(3 \cos^2 \theta - 1)] \end{pmatrix}, \quad (\text{B7})$$

where  $u_A$  is the Cartesian component of the segmental interaction tensor along arm A. These components are related to the strength parameter of the arm-arm interaction for arms of type A by

$$u^{AA} \equiv u_{200}^{AA} = \frac{3}{2}u_A^2, \quad (\text{B8})$$

[see Eq. (B3)] with analogous expressions for  $u^{AB}$  and  $u^{BB}$ . We see from the matrix in Eq. (B7) that  $y$  is a principal axis of the interaction tensor and that to find the other two principal components, it is necessary only to diagonalize a  $2 \times 2$  matrix. This gives the three principal components as

$$u_{xx} = \frac{1}{4} \left[ (u_A + u_B) - 3 \left( u_A^2 + u_B^2 + 4u_A u_B \left( \cos^2 \theta - \frac{1}{2} \right) \right)^{1/2} \right],$$

$$u_{yy} = -\frac{1}{2}(u_A + u_B),$$

$$u_{zz} = \frac{1}{4} \left[ (u_A + u_B) + 3 \left( u_A^2 + u_B^2 + 4u_A u_B \left( \cos^2 \theta - \frac{1}{2} \right) \right)^{1/2} \right]. \quad (\text{B9})$$

The choice of axis labels for the principal components is, in a sense, arbitrary but we shall follow the convention that  $|u_{zz}| > |u_{xx} - u_{yy}|$  and  $(u_{xx} - u_{yy}) > 0$ . With the choice made in Eq. (B9), this would certainly be the case for  $\theta$  close to the extremes of  $0^\circ$  and  $180^\circ$ . The total tensor is traceless [see Eq. (B9)] and so its irreducible spherical components are

$$u_{20} = \sqrt{\frac{3}{32}} \left[ (u_A + u_B) + 3 \left( u_A^2 + u_B^2 + 4u_A u_B \left( \cos^2 \theta - \frac{1}{2} \right) \right)^{1/2} \right]$$

and

$$u_{22} = \frac{3}{8} \left[ (u_A + u_B) - \left( u_A^2 + u_B^2 + 4u_A u_B \left( \cos^2 \theta - \frac{1}{2} \right) \right)^{1/2} \right]. \quad (\text{B10})$$

These give the relative biaxiality as

$$\lambda = \sqrt{\frac{3}{2}} \left[ \frac{(u_A + u_B) - \left( u_A^2 + u_B^2 + 4u_A u_B \left( \cos^2 \theta - \frac{1}{2} \right) \right)^{1/2}}{(u_A + u_B) + 3 \left( u_A^2 + u_B^2 + 4u_A u_B \left( \cos^2 \theta - \frac{1}{2} \right) \right)^{1/2}} \right] \quad (\text{B11})$$

and the major interaction parameter,  $u_{200}$ , as

$$u_{200} (\equiv u_{20}^2) = \frac{3}{32} \left[ (u_A + u_B) + 3 \left( u_A^2 + u_B^2 + 4u_A u_B \left( \cos^2 \theta - \frac{1}{2} \right) \right)^{1/2} \right]^2. \quad (\text{B12})$$

The phase diagram for this single site model is a unique function of the biaxiality parameter  $\lambda$  and the scaled temperature,  $k_B T / u_{200}$  [29,30]. Accordingly, the two expressions for  $\lambda$  and  $u_{200}$  enable us to relate the phase behavior found for different parametrizations of the segmental model. Thus, all of the results should fall on a universal phase diagram when plotted as  $k_B T / u_{200}$  versus  $\lambda$ . This biaxiality parameter is related to the angle between the two arms and their relative anisotropy  $\epsilon^*$  ( $\equiv u_B / u_A \equiv (\epsilon_{BB} / \epsilon_{AA})^{1/2}$ ) by [see Eq. (B11)]

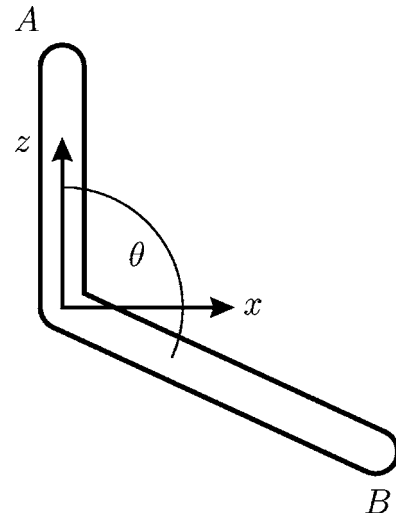


FIG. 5. The axis system for a nonsymmetric V-shaped molecule, as used in Appendix B. Note that the definitions of these axes are different to those used in Fig. 3.

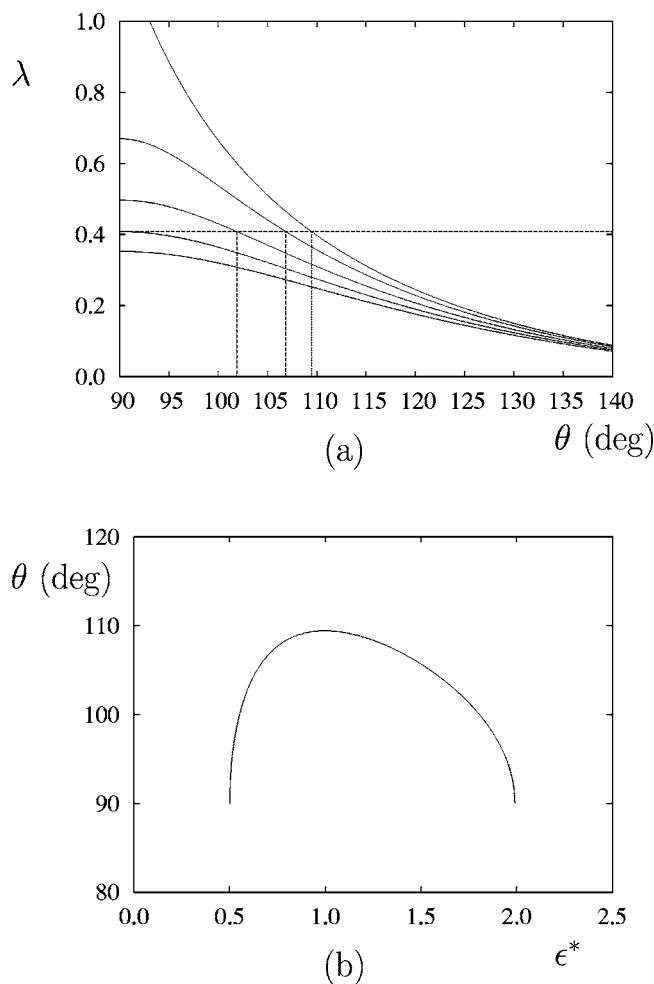


FIG. 6. (a) The dependence of the composite biaxiality parameter  $\lambda$  on the interarm angle  $\theta$  for a selection of values of the relative mesogenic anisotropy  $\epsilon^*$ . From top to bottom:  $\epsilon^* = 1, \sqrt{2}, \sqrt{3}, 2,$  and  $\sqrt{5}$ . (b) The variation of  $\theta$  and  $\epsilon^*$  needed to achieve the optimal composite biaxiality for a nonsymmetric V-shaped molecule.

$$\lambda = \sqrt{\frac{3}{2}} \left[ \frac{(1 + \epsilon^*) - \left(1 + \epsilon^{*2} + 4\epsilon^* \left(\cos^2 \theta - \frac{1}{2}\right)\right)^{1/2}}{(1 + \epsilon^*) + 3 \left(1 + \epsilon^{*2} + 4\epsilon^* \left(\cos^2 \theta - \frac{1}{2}\right)\right)^{1/2}} \right]. \quad (\text{B13})$$

The variation of  $\lambda$  with the angle between the two arms calculated from Eq. (B13) for a selection of the values of the relative anisotropy is given in Fig. 6(a). For the symmetric V-shaped molecule ( $\epsilon^* = 1$ ),  $\lambda$  exhibits a cusp at  $90^\circ$ , but for all other values of  $\epsilon^*$ , the  $\lambda$ - $\theta$  plot passes through a maximum when  $\theta$  is  $90^\circ$ . All of the curves show the expected decrease in  $\lambda$  as  $\theta$  increases from  $90^\circ$  and the molecule becomes more linear. The rate at which  $\lambda$  decreases is largest for the symmetric V-shaped molecule. This dependence of  $\lambda$  on  $\epsilon^*$  is reduced as  $\epsilon^*$  deviates more from unity. The curves for  $\lambda$  shown in Fig. 6(a) reach the value of  $1/\sqrt{6}$ , correspond-

ing to the optimal molecular biaxiality, provided that  $\epsilon^* \leq 2$  (or equivalently  $\epsilon^* \geq \frac{1}{2}$ ); for V-shaped molecules with greater differences in the anisotropies of the arms, this optimal value is not attained. The scaled temperature,  $k_B T/u_{200}$ , is related to  $T^*$  ( $\equiv k_B T/\epsilon_{AA} \equiv 2k_B T/3u_A^2$ ) employed in the simulations by

$$\frac{k_B T}{u_{200}} = 16T^* \left[ (1 + \epsilon^*) + 3 \left(1 + \epsilon^{*2} + 4\epsilon^* \left(\cos^2 \theta - \frac{1}{2}\right)\right)^{1/2} \right]^{-2}. \quad (\text{B14})$$

The expressions for  $\lambda$  and  $u_{200}$  [see Eqs. (B11) and (B12)] adopt interesting limiting values. For example, as the angle between the two arms tends to  $0^\circ$  and  $180^\circ$ , the relative biaxiality vanishes and the major interaction parameter tends to  $(3/2)(u_A + u_B)^2$ . These two limits are equivalent because of the segmental nature of the model and the even rank interactions. When the arms are orthogonal, the biaxiality parameter is given by

$$\lambda = \sqrt{\frac{3}{2}} \frac{\epsilon^*}{(2 - \epsilon^*)}, \quad (\text{B15})$$

and if the arms of the V are equivalent then  $\lambda$  adopts the value of  $\sqrt{3/2}$ , which indicates a uniaxial object. The biaxiality parameter does not adopt the intuitive value of 0 simply because the symmetry axis has not been labeled as the  $z$  axis. In the limit that the anisotropy of one of the arms vanishes, then  $\epsilon^*$  will tend to either 0 or infinity and in this limit, the biaxiality parameter will tend to 0 or  $-\sqrt{3/2}$ , as expected for a uniaxial object. Perhaps of greater interest is the case when  $\epsilon^*$  tends to  $1/2$ , for then  $\lambda$  tends to  $1/\sqrt{6}$ . This value corresponds to the most biaxial object and both theory [30] and simulations [29] agree that the system exhibits a Landau point at which the isotropic phase undergoes a transition directly to the biaxial nematic. Of course, the optimal molecular biaxiality corresponding to the unique value for  $\lambda$  of  $1/\sqrt{6}$  can occur for a range of other combinations of the relative anisotropy of the arms  $\epsilon^*$  and the angle between them  $\theta$  and not only the values ( $\theta = 109.47^\circ$ ,  $\epsilon^* = 1$ ) and ( $\theta = 90^\circ$ ,  $\epsilon^* = 2$ ) just discussed. The relationship between these two parameters giving the optimal biaxiality is

$$\epsilon^* = \frac{1}{4} [5 - 9 \cos^2 \theta \pm ((5 - 9 \cos^2 \theta)^2 - 16)^{1/2}]. \quad (\text{B16})$$

However, not all values of  $\theta$  and  $\epsilon^*$  yield the optimal biaxiality  $\lambda$  of  $1/\sqrt{6}$  and it is possible to find the domains for the two parameters from the constraints that  $\epsilon^*$  must be both real and positive. This constraint on  $\epsilon^*$  gives bounds such that  $\cos^{-1}(1/3) \leq \theta \leq \cos^{-1}(-1/3)$ ; that is, the angle between the arms of the V must be less than or equal to the tetrahedral value of  $109.47^\circ$  and greater than or equal to its supplement,  $70.53^\circ$ . At these two extremes,  $\epsilon^*$  is unity which corresponds to the molecular field theory prediction for the Landau point [4]. In between these two limiting angles, the maximum value of  $\epsilon^*$  is 2, which occurs when the angle between the arms is  $90^\circ$ , as we have already seen. Given the equivalence in our model for the interchange of the labels for the two

arms, the optimal biaxiality when  $\theta=90^\circ$  also occurs when  $\epsilon^* = \frac{1}{2}$ . A plot showing the dependence of  $\epsilon^*$  on  $\theta$  needed to find the Landau point, determined from Eq. (B16), is shown in Fig. 6(b). Note that the optimal biaxiality cannot be achieved for angles larger than the tetrahedral value. This means that the Landau point cannot be shifted to larger angles merely by changing the anisotropy of one (or both) of the arms. The maximum value for  $\epsilon^*$  which can yield a Landau point is 2 and given the symmetry in the model with the interchange of labels, the minimum is  $1/2$ . As  $\epsilon^*$

$\equiv (\epsilon_{BB}/\epsilon_{AA})^{1/2}$ , we note that the relative anisotropy is equal to the square root of the ratio of the nematic-isotropic transition temperatures of the two arms. In other words, the two transition temperatures for the individual arms of the molecule may differ by up to a factor of 4 and the V-shaped molecule will still be able to yield a  $N_B$ -I transition, depending on the angle between the arms. This is clearly a large difference for the transition temperatures and so might offer considerable flexibility in the design of a V-shaped molecule with sufficient biaxiality to yield a biaxial nematic.

- 
- [1] M. J. Freiser, Phys. Rev. Lett. **24**, 1041 (1970).  
 [2] K. Praefcke, B. Kohne, B. GÜdögan, D. Singer, D. Demus, S. Diele, G. Pelzl, and U. Bakowsky, Mol. Cryst. Liq. Cryst. **198**, 393 (1991).  
 [3] J. Malthête, H. T. Nguyen, and A. M. Levelut, J. Chem. Soc., Chem. Commun. **1986**, 1548 (1986); K. Praefcke, B. Kohne, B. Gündogan, D. Demus, S. Diele, and G. Pelzl, Mol. Cryst. Liq. Cryst., Lett. Sect. **7**, 27 (1990); S. Chandrasekhar, G. G. Nair, D. S. Shankar Rao, S. Krishna Prasad, K. Praefcke, and D. Blunk, Curr. Sci. **75**, 1042 (1998).  
 [4] G. R. Luckhurst, Thin Solid Films **393**, 40 (2001).  
 [5] A. Ferrarini, P. L. Nordio, E. Spolaore, and G. R. Luckhurst, J. Chem. Soc., Faraday Trans. **91**, 3177 (1995).  
 [6] P. I. C. Teixeira, A. J. Masters, and B. Mulder, Mol. Cryst. Liq. Cryst. Sci. Technol., Sect. A **323**, 167 (1998).  
 [7] P. J. Camp, M. P. Allen, and A. J. Masters, J. Chem. Phys. **111**, 9871 (1999).  
 [8] Y. Lansac, P. K. Maiti, N. A. Clark, and M. A. Glaser, Phys. Rev. E **67**, 011703 (2003).  
 [9] T. Niori, T. Sekine, J. Watanabe, T. Furukawa, and H. Takezoe, J. Mater. Chem. **7**, 1231 (1996).  
 [10] R. Cai and E. T. Samulski, Liq. Cryst. **9**, 617 (1991); K. J. Semmler, T. J. Dingemans, and E. T. Samulski, *ibid.* **24**, 799 (1998).  
 [11] T. J. Dingemans and E. T. Samulski, Liq. Cryst. **27**, 131 (2000).  
 [12] S. Chandrasekhar, G. G. Nair, D. S. Shankar Rao, and S. Krishna Prasad, Liq. Cryst. **24**, 67 (1998).  
 [13] L. A. Madsen, T. J. Dingemans, M. Nakata, and E. T. Samulski, Phys. Rev. Lett. **92**, 145505 (2004).  
 [14] B. R. Acharya, A. Primak, and S. Kumar, Phys. Rev. Lett. **92**, 145506 (2004).  
 [15] M. Lehmann and J. Levin, Mol. Cryst. Liq. Cryst. **411**, 273 (2004).  
 [16] C. V. Yelamagad, S. Krishna Prasad, G. G. Nair, I. S. Shashikala, D. S. Shankar Rao, C. V. Lobo, and S. Chandrasekhar, Angew. Chem., Int. Ed. **43**, 3429 (2004).  
 [17] P. A. Lebowitz and G. Lasher, Phys. Rev. A **6**, 426 (1972).  
 [18] G. R. Luckhurst and P. Simpson, Mol. Phys. **47**, 251 (1982).  
 [19] R. L. Humphries, P. G. James, and G. R. Luckhurst, Symp. Faraday Soc. **5**, 107 (1971).  
 [20] P. G. de Gennes, *The Physics of Liquid Crystals* (Oxford University Press, Oxford, 1974), p. 27.  
 [21] D. A. Dunmur, and K. Toriyama, in *Physical Properties of Liquid Crystals*, edited by D. Demus, J. W. Goodby, G. W. Gray, H.-W. Spiess, and V. Vill (Wiley-VCH, Weinheim, 1999), Chap. IV.  
 [22] J. Vieillard-Baron, J. Chem. Phys. **56**, 4729 (1972).  
 [23] E. M. Aver'yanov, J. Struct. Chem. **42**, 598 (2001).  
 [24] R. Hashim, G. R. Luckhurst, and S. Romano, Mol. Phys. **53**, 1535 (1984).  
 [25] S. Marcelja, J. Chem. Phys. **60**, 3599 (1974).  
 [26] J. W. Emsley, G. R. Luckhurst, and C. P. Stockley, Proc. R. Soc. London **381**, 117 (1982).  
 [27] G. R. Luckhurst, C. Zannoni, P. L. Nordio, and U. Segre, Mol. Phys. **30**, 1345 (1970).  
 [28] G. R. Luckhurst and S. Romano, Mol. Phys. **40**, 129 (1980).  
 [29] F. Biscarini, C. Chiccoli, P. Pasini, F. Semeria, and C. Zannoni, Phys. Rev. Lett. **75**, 1803 (1995).  
 [30] N. Boccara, R. Mejdani, and L. de Seze, J. Phys. (Paris) **38**, 149 (1977).  
 [31] J. P. Straley, Phys. Rev. A **10**, 1881 (1974).  
 [32] A. M. Sonnet, E. G. Virga and G. E. Durand, Phys. Rev. E **67**, 061701 (2003).  
 [33] R. Berardi and C. Zannoni, J. Chem. Phys. **113**, 5971 (2000).  
 [34] B. Mulder, Phys. Rev. A **39**, 360 (1989).  
 [35] S. Romano, Physica A **339**, 511 (2004).